Universal conductance fluctuations and localization effects in InN nanowires connected in parallel

S. Alagha, S. Estévez Hernández, C. Blömers, T. Stoica, R. Calarco, and Th. Schäpers

Citation: Journal of Applied Physics **108**, 113704 (2010);
View online: https://doi.org/10.1063/1.3516216
View Table of Contents: http://aip.scitation.org/toc/jap/108/11
Published by the American Institute of Physics

Universal conductance fluctuations and localization effects in InN nanowires connected in parallel

S. Alagha, S. Estévez Hernández, C. Blömers, T. Stoica, R. Calarco, and Th. Schäpers[a)]
Institute of Bio- and Nanosystems (IBN-1) and JARA-Fundamentals of Future Information Technology, Forschungszentrum Jülich GmbH, 52425 Jülich, Germany

(Received 2 July 2010; accepted 17 October 2010; published online 3 December 2010)

The low-temperature quantum transport of InN nanowires grown by plasma-assisted molecular beam epitaxy is investigated. Two sets of nanowires with diameters of 100 and 45 nm originating from two different growth runs are studied. Magnetic-field-dependent as well as gate-dependent measurements of universal conductance fluctuations are performed to gain information on the phase-coherence in the electron transport. By analyzing the correlation field and the average fluctuation amplitude a phase-coherence length of several hundred nanometers is extracted for both sets of nanowires at temperatures below 1 K. Conductance fluctuations are also observed when the Fermi wavelength is varied by applying a bias voltage to a back-gate. The results on the electron phase-coherence obtained from the gate-dependent measurements are consistent with the findings from the magnetic field dependent measurements. A considerable damping of the fluctuation amplitude by ensemble averaging is achieved by connecting nanowires in parallel. The suppression of the fluctuation amplitude is studied systematically by measuring samples with different numbers of nanowires. By utilizing the damping of the conductance fluctuations by connecting nanowires in parallel in combination with an averaging over the gate voltage, weak localization effects are resolved. For both sets of nanowires a clear evidence of the weak antilocalization is found, which indicates the presence of spin-orbit coupling. For the spin-orbit scattering length l_{so} values in the order of 100 nm are extracted. © *2010 American Institute of Physics*. [doi:10.1063/1.3516216]

I. INTRODUCTION

Semiconductor nanowires fabricated by a bottom-up approach are very interesting structures to study electron interference effects,[1,2] because here nanoscaled objects can be created without using complex lithographic schemes. If the nanowire is that small, that its dimensions are comparable to the phase-coherence length l_ϕ, i.e., the characteristic length over which the electron phase-coherence is maintained, so-called universal conductance fluctuations can be observed. This phenomenon originates from the fact that in small disordered samples, electron interference effects are not averaged out.[3,4] Under ideal conditions when phase-coherence is maintained in the complete sample the average fluctuation amplitude is found to be *universally* in the order of e^2/h. Conductance fluctuations are observed by varying the magnetic field B or by changing the Fermi energy E_F. In the former case, the electron interference is modified due to the phase-shift caused by the vector potential, whereas in the latter case the interference is altered by changing the Fermi wavelength.

The second type of electron interference phenomena is the weak localization effect. Here, at zero magnetic field contributions of time-reversed electron paths to the quantum-mechanical backscattering amplitude interfere constructively, leading to an increased resistance.[5] The characteristic signature of the weak localization effect is a negative differential magnetoresistance, which originates from the fact that by applying a magnetic field the constructive interference of time-reversed path is gradually suppressed. In contrast, in the presence of spin-orbit coupling the weak antilocalization effect can be observed. The signature of this effect is a resistance minimum at zero field.[5,6] The study of the weak antilocalization is important for the assessment of semiconductor nanostructures for spin electronic applications.

InN nanowires are, in particular, interesting to study the above mentioned electron interference effects, since the electron gas formed at the surface guarantees a low resistance even at small nanowire diameters.[7–15] The presence of the surface electron gas is due to the fact that the surface Fermi level is pinned above the conductance band edge.[16–18]

Here, we report on electron interference effects in the low-temperature transport properties of InN nanowires. Two sets of nanowires with different diameters were investigated. By measuring conductance fluctuations as a function of magnetic field as well as a function of gate voltage information on l_ϕ is gained. Special attention is devoted to the effect of ensemble averaging on the mean amplitude of the conductance fluctuations when different numbers of nanowires are connected in parallel.

In order to resolve weak localization effects in the magnetoconductance of the InN nanowires, the contribution of the conductance fluctuations have to be suppressed sufficiently. One viable way is to average the conductance with respect to E_F.[19] The latter can be changed by means of a gate electrode. According to the *ergodic hypothesis* the averaging by changing E_F is equivalent to the averaging over wires with different impurity configurations as long as the change

[a)]Author to whom correspondence should be addressed. Electronic mail: th.schaepers@fz-juelich.de.

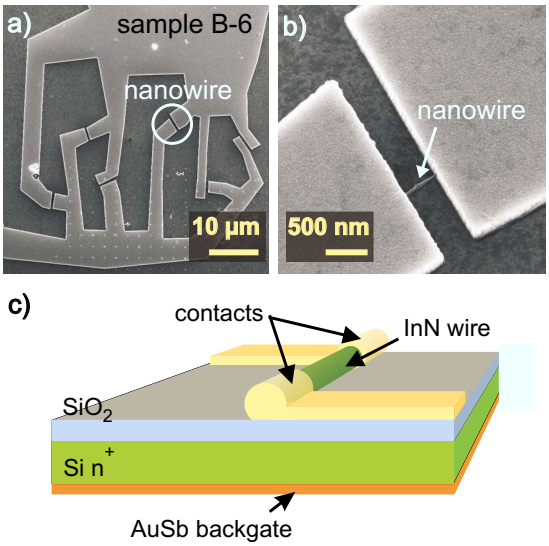

FIG. 1. (Color online) (a) Scanning electron beam micrograph of sample B-6 with six InN wires connected in parallel and (b) detail of a contacted InN nanowire. (c) Schematic illustration of a contacted nanowire. The Si substrate used as a back-gate electrode is isolated from the nanowire by a 100 nm thick SiO_2 layer.

in E_F is equal or bigger than the characteristic correlation energy.[1] Alternatively, the conductance fluctuations can also be suppressed by measuring nanowires connected in parallel, as it was demonstrated on InAs nanowires by Hansen *et al.*[20] Here, we employed both approaches, in order to gain detailed information on weak localization effects. Furthermore, we will address the question if signatures of the weak antilocalization effect can be observed, in order to assess the suitability of InN nanowires for spin electronic applications.

II. EXPERIMENTAL

The InN nanowires were prepared by using plasma-assisted molecular beam epitaxy.[9,21] The wires investigated here were taken from two different growth runs, indicated by the labels A and B. Both types of wires were grown on a Si (111) substrate at a temperature of 475 °C under N-rich conditions. For growth run A, a beam equivalent pressure for In of 3.9×10^{-8} mbar and a growth time of 4 h was chosen, while growth run B was grown at 3.4×10^{-8} mbar for 2 h. The typical diameter d of the wires of growth run A is about 100 nm while the diameter of the wires of growth run B is only 45 nm.

For transport measurements the wires were removed from the original substrate and placed on a highly conductive Si (100) wafer covered by a 100 nm thick SiO_2 insulating layer. Subsequently, single wires or groups of wires were contacted with nonalloyed Ti/Au electrodes patterned by electron beam lithography.[11,14,22] Figures 1(a) and 1(b) show a scanning electron beam micrograph of sample B-6, with six wires connected in parallel and a typical nanowire contacted at its terminals by Ti/Au electrodes, respectively. The n^+-Si substrate was used as a back-gate to control the electron concentration [cf. Fig. 1(c)]. In Table I the parameters and dimensions of the six samples investigated here are summarized.

By measuring the threshold voltage using the conductive substrate as a back-gate a concentration of the surface electron gas of $n_{2d}=1\times10^{13}$ cm^{-2} was estimated at room temperature.[14,23,24] From measurements of the specific resistance a diffusion constant $\mathcal{D}$ of about 680 cm^2/s and 800 cm^2/s was determined for sample series A and B, respectively. In the subsequent analysis a typical contact resistance of 250 Ω for each wire was subtracted from the measured resistance. The contact resistance was extrapolated from resistance measurements of a large number of wires with different contact separations.

The transport measurements were performed in a magnetic field range from 0 to 9 T using a He-3 cryostat. The temperature was varied in the range between 0.4 and 30 K. The magnetic field was oriented perpendicular to the substrate and thus perpendicular to the wire axis. The magnetoresistance was measured by employing a lock-in technique with an ac bias current of 50 nA per wire.

III. RESULTS AND DISCUSSION

The total resistance of the various samples at a temperature of 1 K is summarized in Table I. For each growth run one finds a systematic trend that for increasing number of wires connected in parallel the total resistance decreases. Furthermore, on average the resistance per unit length of a single wire with a value of 850 Ω/μm is found to be smaller for the wires of growth run A, compared to the wires of growth run B, where a value of 2860 Ω/μm was extracted. Assuming a two-dimensional electron gas at the surface the specific resistance is 535 Ω/□ and 810 Ω/□ for the wires of growth run A and B, respectively.

In order to obtain information on the electron phase-coherence length at different temperatures we first analyze

TABLE I. Sample dimensions and characteristic parameters: growth run, number of wires connected in parallel, average wire length $\bar{L}$, average wire diameter $\bar{d}$, total resistance R at 1 K including the contact resistance.

Sample	Growth run	Number of wires	$\bar{L}$ (nm)	$\bar{d}$ (nm)	R (Ω)
A-1	A	1	825 ± 50	100 ± 10	550
A-8	A	8	560 ± 180	100 ± 20	95
B-1	B	1	350 ± 50	45 ± 5	775
B-6	B	6	570 ± 50	45 ± 5	207
B-10	B	10	500 ± 100	45 ± 5	170
B-12	B	12	480 ± 140	45 ± 5	105

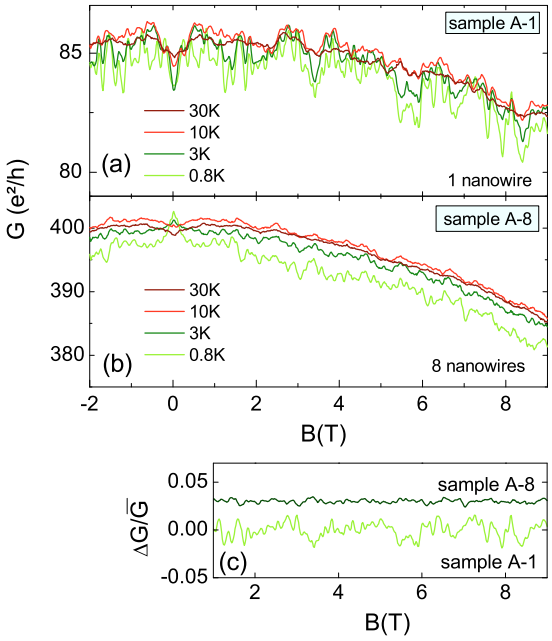

FIG. 2. (Color online) (a) Conductance fluctuations in units of e^2/h for a single wire (sample A-1) at various temperatures in the range from 0.8 to 30 K. (b) Corresponding measurements for a sample with eight wires connected in parallel (sample A-8). (c) Comparison of the conductance fluctuations $\Delta G/\bar{G}$ of samples A-1 and A-8 at 0.8 K. The curve of sample A-8 was shifted by 0.03.

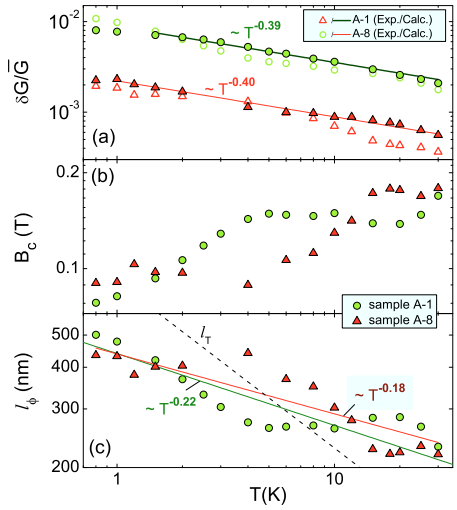

FIG. 3. (Color online) (a) Normalized average amplitude of the conductance fluctuations $\delta G/\bar{G}$ as a function of temperature for sample A-1 (green dots) and sample A-8 (red triangle), respectively. Also shown are the average fluctuation amplitude calculated using Eq. (2) (open symbols), with l_ϕ determined from the correlation field. The full lines show the fitted exponential decrease in $\delta G/\bar{G}$. (b) Correlation field B_c as a function of temperature of sample A-1 and A-8, respectively. (c) Phase-coherence length l_ϕ extracted from B_c. The dashed line corresponds to the thermal length l_T.

the conductance fluctuations measured as a function of magnetic field and gate voltage. Subsequently, weak localization effects will be investigated by employing different averaging schemes.

A. Conductance fluctuations: Magnetic field

At low temperature the conductance G of the InN nanowires fluctuates if the magnetic field is varied. This can be seen in Fig. 2(a), where the magnetoconductance in units of e^2/h of a single nanowire (sample A-1) is shown at various temperatures T. When the temperature is increased from 0.8 to 30 K the average fluctuation amplitude decreases considerably. Since the measurements were performed in a two-terminal configuration the conductance fluctuations are symmetric under magnetic field reversal. In Fig. 2(b) the corresponding magnetoconductance measurements are shown for the sample with eight nanowires connected in parallel (sample A-8). Relating to the total conductance the fluctuations are noticeably smaller. At $T \leq 4$ K a distinct peak is observed at $B=0$. As discussed in more detail in Sec. III C, we attribute this feature to the occurrence of the weak antilocalization effect. In order to illustrate the suppression of the conductance fluctuation by averaging over a number of wires connected in parallel, the normalized conductance fluctuations $\Delta G/\bar{G}$ of both samples are plotted in Fig. 2(c). Here, ΔG corresponds to the total conductance after subtracting the slowly varying background conductance. The conductance $\bar{G}$ is the average conductance measured in the magnetic field range from 1 to 2 T. This range was chosen to avoid contributions of localization effects, which occur close to zero field. Obviously, for sample A-8 the relative fluctuation amplitude is considerably smaller than the corresponding fluctuations of a single wire (sample A-1). In Fig. 2(c) $\Delta G/\bar{G}$ was plotted for a magnetic field range between 1 and 9 T, the range subsequently used to extract the statistical fluctuation parameters. The magnetic field range close to zero field was omitted, in order to exclude possible localization effects.

The properties of the conductance fluctuations are directly connected to the electron phase-coherence in the nanowire. For a detailed analysis the relative average fluctuation amplitude $\delta G/\bar{G}$ was determined at different temperatures, with δG given by the root-mean-square: $\sqrt{\mathrm{var}(\Delta G)}$. The variance is defined by $\mathrm{var}(x)=\langle(x-\langle x\rangle)^2\rangle$, with $\langle\ldots\rangle$ the average over the magnetic field or the Fermi energy. In Fig. 3(a) $\delta G/\bar{G}$ is plotted as a function of T. In the whole temperature range $\delta G/\bar{G}$ of sample A-8 is always smaller than the corresponding values of sample A-1. This observation can be attributed to the above mentioned averaging effect by connecting nanowires in parallel. For N connected wires the variance of the total conductance G_N is given by $\mathrm{var}(G_N)=N\,\mathrm{var}(G_1)$. Here, G_1 is the conductance of a single wire. The average fluctuation amplitude is given by $\delta G_N=\sqrt{\mathrm{var}(G_N)}=\sqrt{N}\delta G_1$. For the average conductance fluctuation with respect to the average total conductance $\bar{G}_N=N\bar{G}_1$ one obtains: $\delta G_N/\bar{G}_N=1/\sqrt{N}\times\delta G_1/\bar{G}_1$. Thus, compared to a single wire the normalized fluctuation amplitude of N wires connected in parallel is reduced by a factor of $\sqrt{N}$. For the two samples of growth run A, we found that $\delta G/G$ differs by a factor of 3.5 at 0.8 K, being close to the expected value of $\sqrt{8}\approx 2.83$.

In order to assess the phase-coherence length l_ϕ, we determined the correlation field B_c, which is a measure for the typical magnetic field scale of the fluctuation. The quantity B_c can be extracted from the autocorrelation function of ΔG

defined by $F(\Delta B)=\langle \Delta G(B+\Delta B)\Delta G(B)\rangle$.[4] The magnetic field corresponding to half maximum $F(B_c)=(1/2)F(0)$ defines B_c. The correlation field as a function of T of samples A-1 and A-8 is shown in Fig. 3(b). Although the values of B_c vary to a certain extend with increasing temperature, on average one finds an increase with T for both samples. From the correlation field the phase-coherence length l_ϕ was extracted by using the following expression:[4,25,26]

$$l_\phi \approx \Phi_0/B_c d, \tag{1}$$

with, $\Phi_0=h/e$ the magnetic flux quantum. The expression given above is obtained in a semiclassical approach, where it is assumed that B_c is inversely proportional to the maximum phase-coherently enclosed area. For quasi-one-dimensional structures with $l_\phi > d$ this area is given by $l_\phi d$. The values of l_ϕ resulting from Eq. (1) are plotted in Fig. 3(c). For both samples l_ϕ decreases from about 500 nm at 0.8 K to slightly above 200 nm at 30 K, following a dependence proportional to $T^{-0.22}$ for sample A-1 and $T^{-0.18}$ for sample A-8.

Theoretically the phase-coherence length is determined from the dephasing time τ_ϕ by $l_\phi=\sqrt{\mathcal{D}\tau_\phi}$. For small energy transfer electron-electron (Nyquist) scattering,[27] which is the relevant contribution at low temperatures,[2] τ_ϕ is proportional to $T^{-2/3}$. Thus l_ϕ is expected to be proportional to $T^{-1/3}$. In agreement to previous measurements,[11] the temperature dependence of l_ϕ is slightly smaller than the theoretically expected dependence. A possible reason for the smaller slope might be that the diffusion constant $\mathcal{D}$, which also affects l_ϕ, increases with temperature. Indeed, as can be seen in Fig. 2, the average conductance and thus $\mathcal{D}$ slightly varies with temperature.

Based on the values of l_ϕ the average fluctuation amplitude δG was calculated by employing the interpolation formula derived by Beenakker and van Houten[26]

$$\delta G = \alpha \frac{e^2}{h}\left(\frac{l_\phi}{L}\right)^{3/2}\left[1+\frac{9}{2\pi}\left(\frac{l_\phi}{l_T}\right)^2\right]^{-1/2}. \tag{2}$$

Here, the thermal diffusion length l_T is defined by $\sqrt{\hbar\mathcal{D}/k_BT}$. The formula is valid in the transition range, where l_ϕ is in the same order as l_T. That the latter condition is fulfilled can be inferred from Fig. 3(c). As can be seen in Fig. 3(a), for both samples the decrease in the $\delta G/G$ is well reproduced by the calculated values by using $\alpha=2.4$. The exponential decrease in $\delta G/G$ shown in Fig. 3(a) of $\sim T^{-0.39}$ and $T^{-0.41}$ for sample A-1 and A-8, respectively, are slightly smaller than expected from Eq. (2) but consistent with the experimentally observed decrease of l_ϕ smaller than $T^{-1/3}$.

For the wires of growth run B one can infer from Figs. 4(a)–4(d), that the conductance of the single wire (sample B-1) and the six, ten, and 12 wires connected in parallel (samples B-6, B-10, and B-12) fluctuate on a considerably longer magnetic field scale compared to the measurements of the wires of growth run A. This is a consequence of the relation expressed by Eq. (1) where one expects for a comparable phase-coherence length a larger correlation field if the diameter is smaller. When the temperature is increased to 30 K the conductance fluctuations are almost suppressed completely. The decrease in the conductance fluctuation amplitude with increasing temperature can be seen clearly in the color scale plot of the conductance fluctuations ΔG of sample B-10 shown in Fig. 4(e). Similar to the previously discussed samples A-1 and A-8 $\delta G/\bar{G}$ decreases if the number of wires is increased. Compared to the single wire, for six, ten, and 12 wires $\delta G/\bar{G}$ is smaller by a factor of about 0.37, 0.32, and 0.24 at temperatures below 1.0 K which is close to the expected decrease by $1/\sqrt{N}$ of 0.41, 0.32, and, 0.29, respectively [cf. Fig. 5(inset)].

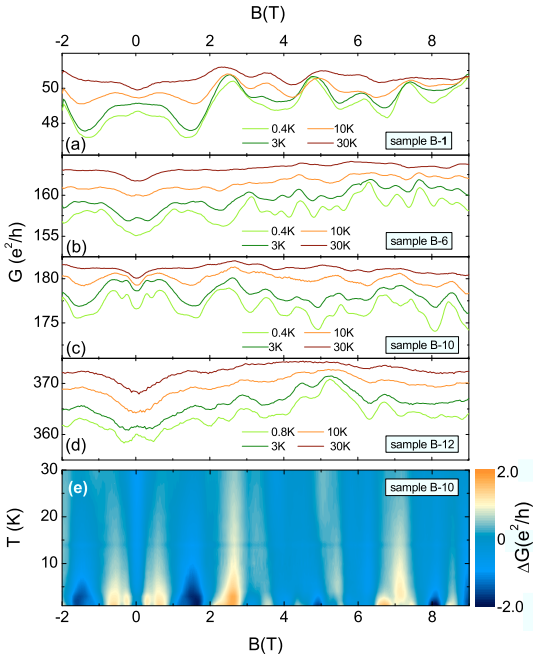

FIG. 4. (Color online) Conductance fluctuations normalized to e^2/h at various temperatures of 0.4, 3, 10, and 30 K for samples with different numbers of wires connected in parallel: (a) sample B-1, (b) B-6, (c) B-10, and (d) B-12. Color scale plot of the conductance fluctuations ΔG of sample B-10 as function of magnetic field and temperature. ΔG was determined by subtracting the slowly varying background conductance.

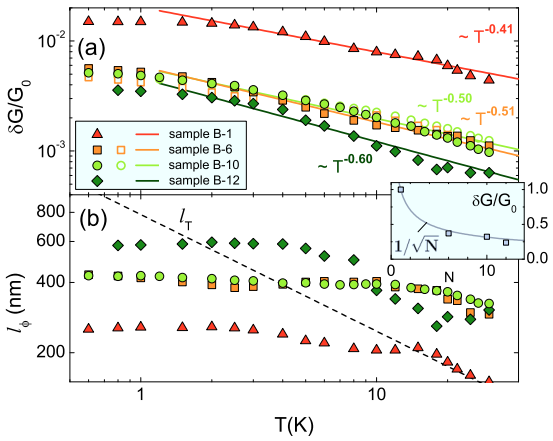

FIG. 5. (Color online) (a) $\delta G/\bar{G}$ as a function of temperature for a single wire (sample B-1) as well as for six, ten, and 12 wires (samples B-6, B-10, and B-12) connected in parallel. The open symbols represent the calculated values for B-6 and B-10 using Eq. (2). The full lines show the fitted exponential decrease in $\delta G/\bar{G}$. (b) l_ϕ as a function of T for samples B-1, B-6, B-10, and B-12. The dashed line represents the thermal length l_T. The inset shows the decrease in $\delta G/\bar{G}$ with increasing number of wires N for T below 1 K.

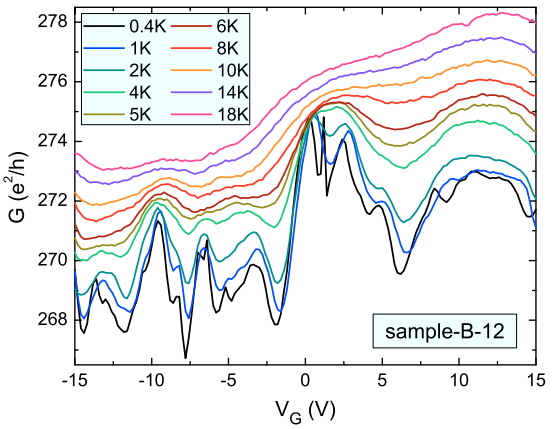

FIG. 6. (Color online) Conductance G of sample B-12 as a function of gate voltage for various temperatures.

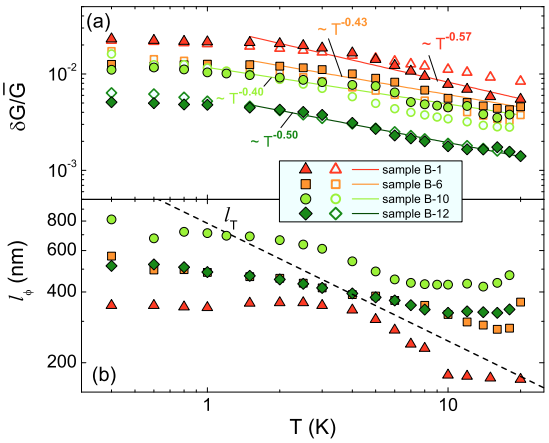

FIG. 7. (Color online) (a) Normalized conductance fluctuations averaged over V_G as a function of temperature for a single wire (sample B-1) as well as for six, ten, and 12 wires (samples B-6, B-10, and B-12) connected in parallel. The open symbols represent the calculations using Eq. (2). The full lines show the exponential decrease of $\delta G/G_0$. (b) Respective phase-coherence length as a function of temperature. The dashed line represents the thermal length l_T.

The decrease in $\delta G/\bar{G}$ with temperature is shown in Fig. 5(a). As one can see here, for all four samples the exponential decrease of $\delta G/\bar{G}$ with temperature is close to the one expected from Eq. (2). Only for sample B-6 and B-10 we were able to extract l_ϕ from B_c. For the other two samples (B-1, B-12) B_c could not be determined reliably which is attributed to the large fluctuation period compared to the measurement range of 0–9 T. The corresponding values of l_ϕ obtained by applying Eq. (1) are shown in Fig. 5(b). For both samples l_ϕ is about 400 nm at low temperature ($T<10$ K) and thus comparable to the values estimated for the sample with the larger diameter (growth run A). The exponential decrease in l_ϕ with temperature can be approximated by $T^{-0.10}$, which is somewhat smaller that theoretically expected. Based on l_ϕ the average fluctuation amplitude was calculated using Eq. (2). As one can see in Fig. 5(a), the calculated values of $\delta G/\bar{G}$ closely follow the experimental values for $\alpha=1.2$. For the remaining two samples (B-1, B-12) B_c, l_ϕ was determined instead from the measurements of $\delta G/\bar{G}$ by applying Eq. (2) and using $\alpha=1.2$. As can be seen in Fig. 5(b) for sample B-12 a maximum value of about 600 nm was estimated for l_ϕ at low temperatures, while for sample B-1 a value of about 300 nm was reached. We attribute the large spread of values between the different samples of this set to the uncertainties in the determination of B_c and δG owing to the large magnetic field scale of the fluctuations.

B. Conductance fluctuations: gate voltage

So far we presented measurements of the conductance fluctuations as a function of magnetic field. Alternatively fluctuations can also be observed when the Fermi energy and thus the Fermi wavelength is varied by means of a gate voltage V_G. In Fig. 6, this is shown exemplarily for sample B-12 where the gate voltage dependence of the conductance is plotted at various temperatures. For these measurements, the n^+ Si substrate was employed as a global back-gate to vary the electron concentration in all nanowires simultaneously. As one can see in Fig. 6, owing to the large electron concentration in the surface electron gas only a slight carrier depletion is achieved indicated by the small decrease in the average conductance with decreasing V_G. The accessible gate voltage range was limited by the maximum allowed leakage current of a few nanoamperes.

The temperature dependence of the normalized conductance fluctuation amplitude $\delta G/G_0$ of all samples of growth run B is shown in Fig. 7(a), with G_0 the conductance at $V_G=0$. For the determination of δG the linear background due to the change in electron concentration with V_G was subtracted. In accordance with the measurements as a function of magnetic field we find that with increasing number of wires $\delta G/G_0$ is reduced. For exponential decrease with temperature we obtained exponents in the range between -0.43 and -0.57. A comparison of the values $\delta G/G_0$ shown in Fig. 5(a) reveals that the average fluctuation amplitudes are systematically larger for the gated measurements performed at zero field. Such a behavior is predicted by theory,[28,29] where the fluctuation amplitudes δG at $B=0$ are expected to be larger by a factor of $\sqrt{2}$ compared to the corresponding amplitudes extracted from magnetic field dependent measurements for $B>B_c$. For our four samples we found amplitudes larger by a factor between 1.4 and 2.3 at 1 K. Based on the assumption that E_F is proportional to n_{2d} the phase-coherence length was estimated by using the expression[19]

$$l_\phi = \sqrt{2m^* D V_{Th}/\hbar n_{2d} V_c}. \tag{3}$$

Here, V_{Th} is the threshold voltage, which was extrapolated to be about -250 V. The correlation voltage V_c of the gate voltage dependent fluctuations was calculated in analogy to the determination of B_c. For the effective mass we assumed a value of $m^*=0.07\ m_e$.[30]

The phase-coherence length as a function of temperature calculated by means of Eq. (3) is given in Fig. 7(b). One finds that the values obtained here are close to the values extracted from the magnetic field dependent fluctuation measurements. In the light of the relatively rough estimates of some sample parameters, i.e., V_{Th} and n_{2d}, no better matching can be expected. In general one finds a decrease of l_ϕ

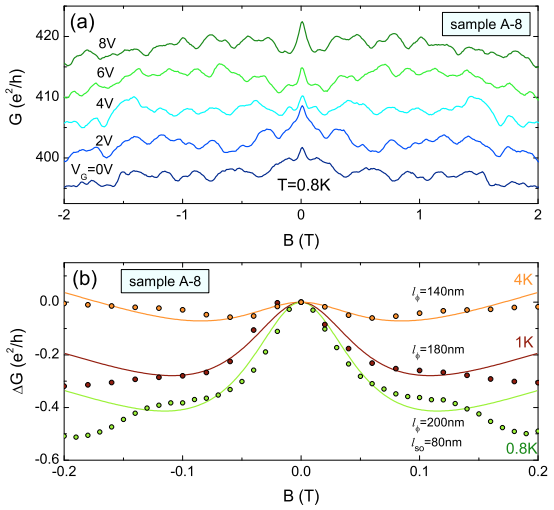

FIG. 8. (Color online) (a) Magnetoconductance of sample A-8 at 0.8 K at a gate voltage of 0, 2, 4, 6, and 8 V, respectively. (b) Correction of the magnetoconductance ΔG of sample A-8 averaged over different gate voltages at 0.8 K, 1.0 K and 4.0 K, respectively. Here, the zero field conductance was subtracted from the total conductance.

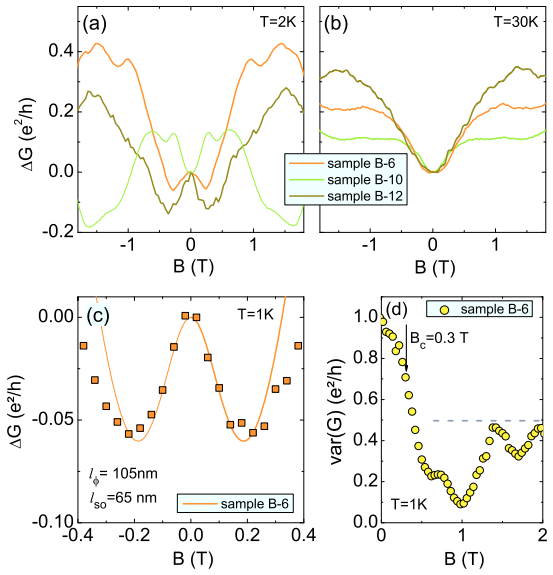

FIG. 9. (Color online) (a) and (b) Magnetoconductance ΔG of samples B-6, B-10, and B-12 after subtracting the zero field conductance at a temperature of 2 K and at 30 K, respectively. (c) ΔG vs B of sample B-6 after averaging over different gate voltages. The full line shows the fit to the experimental data. (d) var(G) in units of e^2/h of the gate voltage dependent fluctuations as a function of B.

with temperatures. As one can infer from Fig. 7(a), a good agreement between the calculated values of $\delta G/G_0$ and the experimental values is obtained for all four samples.

C. Localization effects

Owing to the distinct conductance fluctuations of single nanowires, signatures related to localization effects are masked almost completely. This can be seen in Fig. 2(a), where no distinguished feature is resolved around zero magnetic field for sample A-1. Yet with increasing number of nanowires connected in parallel, the conductance fluctuation amplitude is attenuated, so that in this case localization effects are revealed [cf. Fig. 2(b)]. In order to resolve these features even better, a further smoothing was performed by averaging magnetoconductance traces measured at fixed back gate voltages. The set of magnetoconductance measurements at gate voltages between 0 and +8 V for $T=0.8$ K is shown in Fig. 8(a). As can be seen in Fig. 8(b), the magnetoconductance correction ΔG, obtained after averaging all five traces, shows a clear conductance peak at zero magnetic field. Here, ΔG is given by $G-G_0$ with G_0 the zero field conductance. With increasing temperature, the peak height decreases, while the remains of the conductance fluctuations diminish further. We attribute the conductance peak to the weak antilocalization effect.[5,6] Previously, indications for spin-orbit coupling in InN nanowires were found in single InN nanowires, where the averaging was only performed over the gate voltage.[19] However, in the present case by making use of two averaging effects, i.e., over different samples as well as various gate voltages, a better suppression of fluctuation contributions is achieved. In order to gain information about the spin-orbit scattering length l_{so} being a measure of the spin-orbit coupling strength, the experimental curves were fitted by curves based on the model of Kettemann and Wenk.[31,32] At 0.8 K we obtained $l_{so}=80$ nm and $l_\phi=200$ nm, from the fit. The latter value is consistent with the one extracted from the analysis of the conductance fluctuations. From the fit to the corresponding measurements at 1.0 K a lower value of l_ϕ was obtained while l_{so} remained the same as before. At a temperature of 4 K only a small conductance peak remained, here the fitting resulted in $l_\phi=140$ nm with $l_{so}=80$ nm as before.

In Figs. 9(a) and 9(b) ΔG of samples B-6, B-10, and B-12 is shown at 2 K and at 30 K, respectively. Obviously, at 2 K no clear feature attributed to localization effects can be resolved, which can be explained by the masking effect of the conductance fluctuations. At higher temperatures of 30 K all three samples reveal a clear minimum in the conductance at zero magnetic field, which can be attributed to the weak localization effect.

In order to minimize the detrimental effect of the conductance fluctuations an additional averaging over the gate voltage was performed for sample B-6. The resulting magnetoconductance is shown in Fig. 9(c). Owing to the averaging a damping of the conductance fluctuations by a factor of about 5 was achieved, while the peak height at zero field remained approximately the same. The fit to the experimental data resulted in $l_\phi=105$ nm and $l_{so}=65$ nm. The phase-coherence length is smaller than l_ϕ extracted from the analysis of the conductance fluctuations. We attribute this discrepancy to the fact that both underlying theoretical approaches do not account for the tubular geometry of the surface electron gas of the InN nanowires.

For the measurements of the conductance fluctuations as a function of the gate voltage described in Sec. III B we found that the average fluctuation amplitude $\delta G/G_0$ at $B=0$ is systematically larger than the corresponding value for the magnetic field dependent measurements. In Fig. 9(d) the variance var(G) of the gate-voltage dependent fluctuations at a fixed magnetic field of sample B-6 is plotted as a function of B. As one can clearly see, var(G) decreases when a mag-

netic field is applied. This behavior can be explained by the fact that by applying a magnetic field the contribution of the cooperon channel to the conductance fluctuations is completely suppressed due to the breaking of the time-reversal symmetry, so that only electron correlations in the diffusion channel remain.[28,29] In fact, as can be seen in Fig. 9(d), var(G) drops significantly, when B is increased. The characteristic field where the drop of var(G) occurs is the correlation field B_c, which is about 0.3 T for this sample.

IV. CONCLUSIONS

In conclusion, the low temperature phase-coherent electron transport was investigated for two sets of InN nanowires. For both types of nanowires it was found that l_ϕ is in the order of several hundred nanometers at temperatures below 1 K. For the extraction of l_ϕ a model was utilized which was originally set-up for wire structures based on two-dimensional electron gases. Therefore, there might be some uncertainty contained in the values of l_ϕ, due to the cylindrical geometry of the nanowires. Nevertheless, the expected temperature-dependence of the average amplitude predicted by the model of Beenakker and van Houten[26] could be well reproduced by our data. For the nanowires with the smaller diameter a noticeable larger magnetic field scale of the conductance fluctuation was found, which could be explained by the larger correlation field being inversely proportional to the radius. By connecting a number of nanowires in parallel a damping of the fluctuation amplitude was achieved, which closely followed the expected attenuation by $1/\sqrt{N}$. By employing a back gate electrode, conductance fluctuations were also observed when the gate bias voltage was varied. The results on the phase-coherence length were consistent with the results obtained from the field-dependent measurements. In order to clearly resolve weak localization effects, two averaging methods had been employed simultaneously, i.e., the averaging by measuring wires connected in parallel and the averaging of the conductance over the gate voltage. For nanowires of both growth runs evidence of weak antilocalization was observed, which indicates the presence of spin-orbit coupling. For the wires of the first growth run a spin-orbit scattering length of approximately 80 nm was extracted from a fit to a theoretical model, while for the second set of wires l_{so} of about 65 nm was calculated. Details on the physical origin of the spin-orbit coupling effect is not clear, yet. Possible mechanisms are the Rashba effect due to the surface accumulation layer[33] or the spin-orbit coupling due the lack of crystal inversion symmetry.[34,35] The presence of spin-orbit coupling make these nanowires interesting for applications in the field of spin electronic.

We are grateful to D. Grützmacher for fruitful discussions and comments to the manuscript. We thank K.-H. Deussen and H. Kertz for the support during the wire growth and during the measurements.

[1] C. W. J. Beenakker and H. van Houten, in *Solid State Physics*, edited by H. Ehrenreich and D. Turnbull (Academic, New York, 1991), Vol. 44, p. 1.
[2] J. J. Lin and J. P. Bird, J. Phys.: Condens. Matter **14**, R501 (2002).
[3] B. Altshuler, Pis'ma Zh. Eksp. Teor. Fiz. **41**, 530 (1985) [JETP Lett. **41**, 648 (1985)].
[4] P. A. Lee, A. D. Stone, and H. Fukuyama, Phys. Rev. B **35**, 1039 (1987).
[5] G. Bergmann, Phys. Rep. **107**, 1 (1984).
[6] S. Hikami, A. I. Larkin, and Y. Nagaoka, Prog. Theor. Phys. **63**, 707 (1980).
[7] C. H. Liang, L. C. Chen, J. S. Hwang, K. H. Chen, Y. T. Hung, and Y. F. Chen, Appl. Phys. Lett. **81**, 22 (2002).
[8] C.-Y. Chang, G.-C. Chi, W.-M. Wang, L.-C. Chen, K.-H. Chen, F. Ren, and S. J. Pearton, Appl. Phys. Lett. **87**, 093112 (2005).
[9] T. Stoica, R. J. Meijers, R. Calarco, T. Richter, E. Sutter, and H. Lüth, Nano Lett. **6**, 1541 (2006).
[10] R. Calarco and M. Marso, Appl. Phys. A: Mater. Sci. Process. **87**, 499 (2007).
[11] C. Blömers, Th. Schäpers, T. Richter, R. Calarco, H. Lüth, and M. Marso, Appl. Phys. Lett. **92**, 132101 (2008).
[12] C. Blömers, Th. Schäpers, T. Richter, R. Calarco, H. Lüth, and M. Marso, Phys. Rev. B **77**, 201301 (2008).
[13] F. Werner, F. Limbach, M. Carsten, C. Denker, J. Malindretos, and A. Rizzi, Nano Lett. **9**, 1567 (2009).
[14] T. Richter, H. Lüth, T. Schäpers, R. Meijers, K. Jeganathan, S. E. Hernandez, R. Calarco, and M. Marso, Nanotechnology **20**, 405206 (2009).
[15] J. Segura-Ruiz, N. Garro, A. Cantarero, C. Denker, J. Malindretos, and A. Rizzi, Phys. Rev. B **79**, 115305 (2009).
[16] I. Mahboob, T. D. Veal, C. F. McConville, H. Lu, and W. J. Schaff, Phys. Rev. Lett. **92**, 036804 (2004).
[17] C. G. V. de Walle and D. Segev, J. Appl. Phys. **101**, 081704 (2007).
[18] T. Richter, Ch. Blömers, H. Lüth, R. Calarco, M. Indlekofer, M. Marso, and Th. Schäpers, Nano Lett. **8**, 2834 (2008).
[19] G. Petersen, S. Estévez Hernández, R. Calarco, N. Demarina, and Th. Schäpers, Phys. Rev. B **80**, 125321 (2009).
[20] A. E. Hansen, M. T. Björk, C. Fasth, C. Thelander, and L. Samuelson, Phys. Rev. B **71**, 205328 (2005).
[21] T. Stoica, R. Meijers, R. Calarco, T. Richter, and H. Lüth, J. Cryst. Growth **290**, 241 (2006).
[22] R. Calarco, M. Marso, T. Richter, A. I. Aykanat, R. Meijers, A. v.d. Hart, T. Stoica, and H. Lüth, Nano Lett. **5**, 981 (2005).
[23] J. Noborisaka, T. Sato, J. Motohisa, S. Hara, K. Tomioka, and T. Fukui, Jpn. J. Appl. Phys., Part 1 **46**, 7562 (2007).
[24] S. Dayeh, D. P. Aplin, X. Zhou, P. K. Yu, E. Yu, and D. Wang, Small **3**, 326 (2007).
[25] P. A. Lee and A. D. Stone, Phys. Rev. Lett. **55**, 1622 (1985).
[26] C. W. J. Beenakker and H. van Houten, Phys. Rev. B **37**, 6544 (1988).
[27] B. L. Altshuler, A. G. Aronov, and D. E. Khmelnitsky, J. Phys. C **15**, 7367 (1982).
[28] B. Altshuler and B. Shklovskii, Zh. Eksp. Teor. Fiz. **91**, 220 (1985) [Sov. Phys. JETP **64**, 127 (1986)].
[29] A. D. Stone, Phys. Rev. B **39**, 10736 (1989).
[30] I. Vurgaftman and J. R. Meyer, J. Appl. Phys. **94**, 3675 (2003).
[31] S. Kettemann, Phys. Rev. Lett. **98**, 176808 (2007).
[32] P. Wenk and S. Kettemann, Phys. Rev. B **81**, 125309 (2010).
[33] Y. Bychkov and E. I. Rashba, J. Phys. C **17**, 6039 (1984).
[34] G. Dresselhaus, Phys. Rev. **100**, 580 (1955).
[35] E. I. Rashba, Fiz. Tverd. Tela (Leningrad) **2**, 1224 (1960) [Sov. Phys. Solid State **2**, 1109 (1960)].